UNIVERSITY HONORS PROGRAM

SENIOR PROJECT - APPROVAL

Name: William H. Grover

College: Arts & Sciences Department: Chemistry

Faculty Mentor: James Q. Chambers

PROJECT TITLE: "Interdigitated Array Electrode Sensors: Their Design, Efficiency, and Applications"

I have reviewed this completed senior honors thesis with this student and certify that it is a project commensurate with honors level undergraduate research in this field.

Signed: James Q Chambers, Faculty Mentor

Date: 10 May, 1999

Comments (Optional):

Interdigitated Array Electrode Sensors:

Their Design, Efficiency, and Applications

University Honors Senior Project

Will Grover

Outline

I. Overview of Interdigitated Electrode Research

II. Sensor Applications for Interdigitated Electrodes

- A. Generic sensor
- B. Mechanical interdigitated electrode sensors
- C. Chemical interdigitated electrode sensors
  - 1. Capacitive chemical sensors
  - 2. Resistive chemical sensors
- D. Surface acoustic wave (SAW) sensors

III. Efficiency of Interdigitated Electrode Sensor Designs

- A. Design of the generic interdigitated electrode sensor
- B. Unoptimized sensing material in the generic interdigitated electrode sensor
- C. Theory behind unoptimized sensing areas
- D. Introduction of the efficiency statement for interdigitated electrode sensors
- E. Application of the efficiency statement for analysis and improvement of the generic interdigitated electrode sensor
  - 1. Efficiency analysis of the unimproved generic interdigitated electrode sensor
  - 2. Efficiency analysis of the improved generic interdigitated electrode sensor
- F. Dimensional optimization of interdigitated electrode sensors

1. Dimensional optimization of the generic interdigitated electrode sensor

2. Introduction of the maximum possible efficiency

G. Introduction of the optimization term

H Efficiency and dimensional optimization as tools for sensor improvement

IV. Presentation and Analysis of Novel Interdigitated Electrode Sensor Designs

A. Electrodes with non-negligible resistance

B. Circuit model of the parallel electrode chemical sensor

C. The tapered gap

D. Novel interdigitated electrode sensor design

1. Circular interdigitated electrode sensor

2. Hexagonal array interdigitated electrode sensor

I. Overview of Interdigitated Electrode Research.

Although not officially a part of any single research project, my research of the efficiency and design of interdigitated electrode chemical sensors spans two research projects and two years. While using an automated fluid deposition robot to dispense dots of polyaniline sensing layers onto the gate regions of chemically-sensitive field effect transistor (CHEMFET) sensors, I realized that the instrument could be programmed to dispense conductive epoxy in the pattern of a crude interdigitated electrode. Once the electrodes were deposited onto an insulating substrate, the same instrument could then be used to dispense a dot of sensing layer on top of the interdigitated electrode array. I was successful in fabricating several crude interdigitated electrode sensors in this manner; the sensors were given a polyaniline sensing layer and found to have reasonably good responses and recoveries to fairly low concentrations of gaseous analytes such as ammonia and hydrogen in nitrogen. Subsequent research into interdigitated electrodes suggested that while many fields of study routinely use interdigitated electrodes, relatively little has been said about the design of the interdigitated electrodes commonly used. This research project hopes to fill that void somewhat by introducing mathematical statements for efficiency and other terms that define an interdigitated electrode sensor's relative and absolute quality as a sensor. To apply these principles of efficiency, several improvements upon traditional interdigitated electrode designs are also presented.

II. Sensor Applications for Interdigitated Electrode Arrays.

Interdigitated electrode arrays are pervasive devices in modern electronics. While concentrating upon the application of these devices as resistive and capacitive chemical sensors, other important sensor applications for interdigitated electrode arrays will be examined in an effort to convey the importance of these devices.

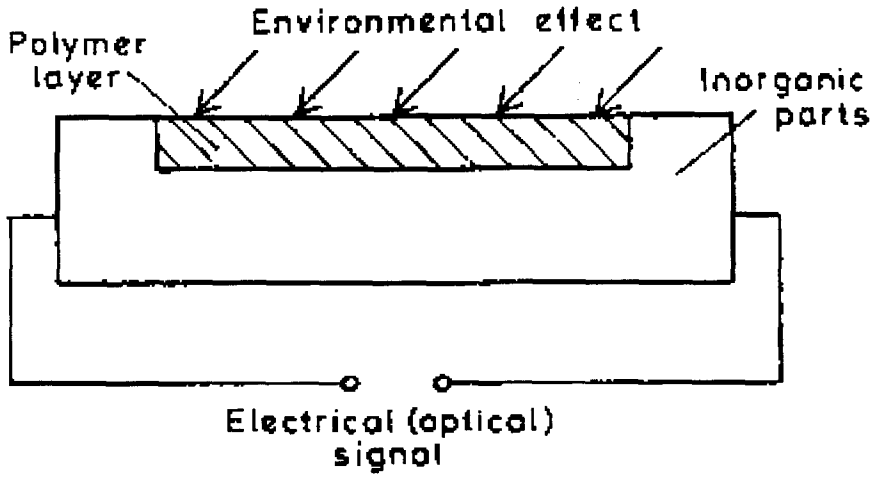
II.A *A generic sensor.*

Harsanyi[1] presents a generic model of a polymer sensor that is nonetheless applicable to practically any sensor, including those with interdigitated electrodes. A graphical model of this generic sensor is shown in Figure 1. The polymer layer shown in Figure 1 may be replaced with any material sensitive to chemicals, humidity, force, acceleration, or any of a host of other substances or phenomena summarized as environmental effects. The inorganic parts in Figure 1 include the interfaces between the sensing layer and the electrical signal. Often these interfacial structures take the form of interdigitated electrodes, which, in a broad sense, maximize the area of contact between the sensing layer and the electrical signal being measured.

II.B *Mechanical interdigitated electrode sensors.*

Although the main focus of this work lies in analyzing the efficiency of interdigitated electrodes in chemical sensor applications, the large range of non-chemical sensor applications for interdigitated electrodes merits some mention here. Mechanical pressure sensors using interdigitated electrodes, for example, find use in thin membrane

Figure 1: Generic polymer-based sensor[1]



switches for electronic devices. Such a sensor consists of an interdigitated electrode patterned on an insulating plastic carrier which in turn rests upon a conductive plate or a semiconductive polymer layer[2]. A typical device is shown in Figure 2. As the force *F* on the sensor increases, the area of contact between the interdigitated electrodes and the semiconductive layer increases. The resistance between the two interdigitated electrodes thereby decreases as the force increases. Semiconductive polymers are favored over ordinary conductive (metal) backings because the conductivity of such polymers change with applied force[2]. The inclusion of a semiconductive polymer layer resting on the interdigitated electrode array adds an additional amount of sensitivity and range to the force sensor. When these force sensors are used in electronic devices as membrane switches, a finger provides the force necessary to press a conductive polymer thick-film (PTF) against an interdigitated electrode array, thereby completing a circuit between the two interdigitated electrodes. A diagram of a typical interdigitated electrode membrane switch is shown in Figure 3. In Figure 3(a), the alternating interdigitated electrodes (labeled "pads") are isolated on an insulating polymer sheet and no current flows between them, so the switch is in the open position. As the switch is pressed in Figure 3(b), a conductive polymer sheet is pressed against the interdigitated electrodes and current flows between them, thereby closing the switch. I constructed a similar force sensor by resting a partially-conductive iron oxide film on two parallel electrodes and measuring the change in resistance across the electrodes as a function of applied force.

Figure 2: Tactile sensor with a polymer force-sensitive resistor[2]

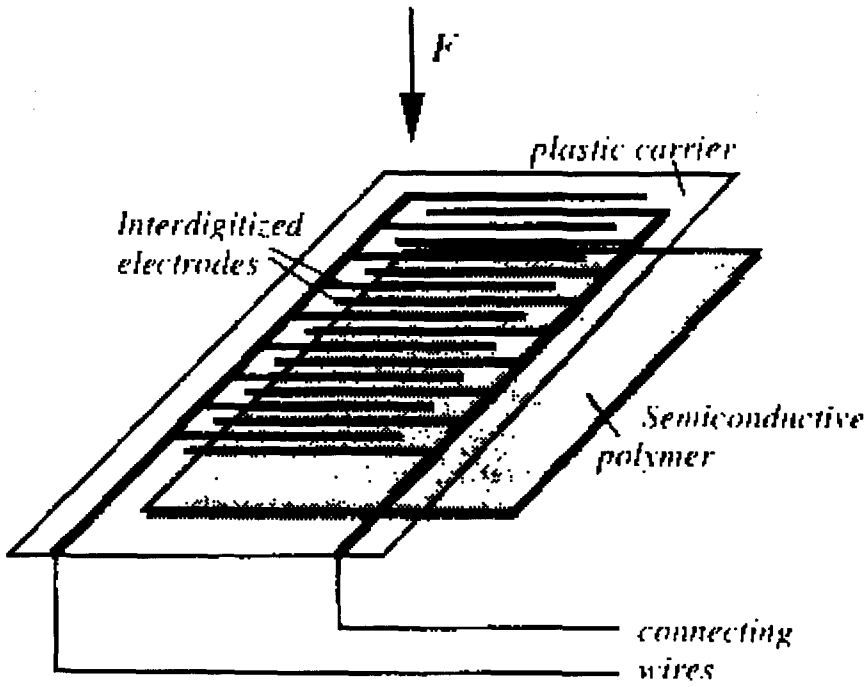
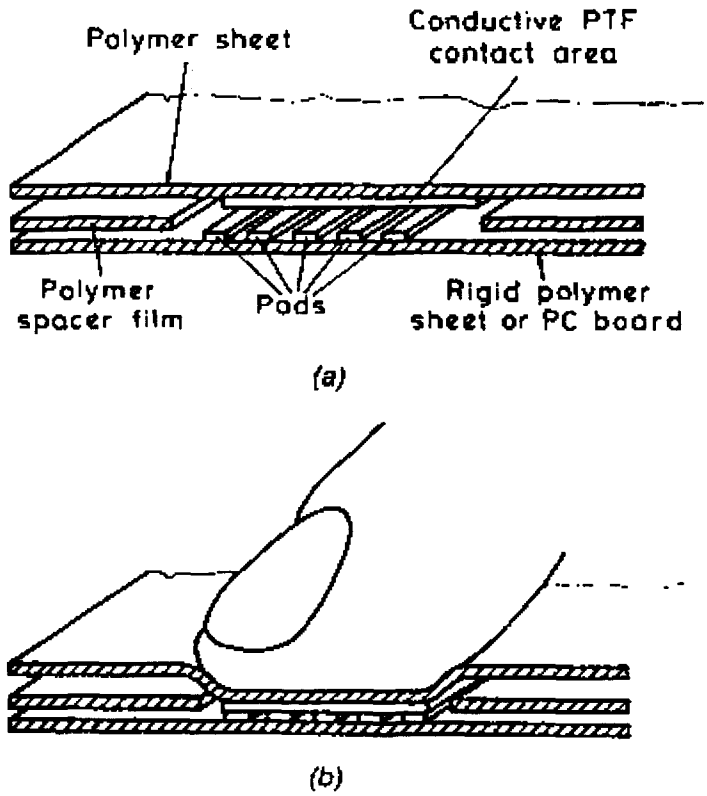


Figure 3: Membrane switch utilizing interdigitated electrode contacts[1]



II.C *Chemical interdigitated electrode sensors.*

Chemical sensors constructed using interdigitated electrodes usually fall into one of two distinct categories: capacitive sensors and resistive sensors. Both types of sensors capitalize upon the aforementioned principal benefit of interdigitated electrodes—increased contact area between the sensing material and the sensor circuitry—but they differ in the role of the chemical sensing layer. In capacitive chemical sensors, the sensing layer acts as the dielectric between two parallel interdigitated electrodes; in resistive sensors, the sensing layer acts as a resistor between two electrodes in an interdigitated pattern. As a result, the reaction of a capacitive sensor to stimuli is measured by a change in the capacitance of the sensor, and the reaction of a resistive sensor to stimuli is measured by a change in resistance of the sensor. In addition to discussing these two primary types of chemical interdigitated electrode sensors, the surface acoustic wave or SAW sensor will be examined as a unique hybrid chemical sensor that uses interdigitated electrodes.

II.C.1 *Capacitive chemical sensors.*

An early use for capacitive sensors in general (both interdigitated electrode types as well as earlier parallel-plate capacitors) was for relative humidity measurement. A capacitor consisting of two (or more) parallel plates or electrodes separated by an ambient air dielectric will function as a humidity sensor because the electrical permitivity κ of air is a function of the relative percent humidity H of the air, as shown in Equation 1.

$$\kappa = 1 + \frac{211}{T}\left(P + \frac{48P_s}{T}H\right)10^{-6} \qquad (1)$$

where T and P are the absolute temperature in Kelvin and pressure in mmHg of the air, respectively, and P_s is the pressure of saturated water vapor at temperature T [2]. A capacitive humidity sensor measures the electrical permitivity κ of ambient air. An actual value for κ need not be determined since the relative humidity H of the ambient air may be directly correlated with the measured capacitance C_h of the sensor device. This relationship is expressed in Equation 2

$$C_h = C_0(1 + \alpha_h H) \tag{2}$$

where C_h is the measured capacitance of the sensor, C_0 is the capacitance when absolutely dry air is used as the dielectric, α_h is a proportionality constant, and H is the relative humidity[1]. Interdigitated electrodes are particularly well-suited for use in capacitive humidity sensors; the lengthy, serpentine gap between electrodes in an interdigitated electrode provides a large region for air to function as a dielectric. In fact, the gap may be modeled as a long chain of individual *capacitors* arranged in parallel. The merits and implications of this model will be discussed later. If sensors for analytes other than water vapor are desired, an insulating chemically-sensitive layer or thin film may be deposited over the interdigitated electrode array. This layer functions as the dielectric in the resulting interdigitated electrode capacitor; the dielectric constant of the sensing layer changes as the layer is exposed to different analytes in different concentrations, and the capacitance is measured as a function of analyte concentration. Note that the sensing layer must be essentially nonconductive since the flow of current

across the layer would discharge the interdigitated electrode capacitor and make capacitance measurements impossible; such a device would then be a *resistive sensor*, discussed later. Figure 4(a) shows a capacitive thin-film chemical sensor integrated with two temperature sensors on the same insulating substrate. Figure 4(b) shows a cross section of the sensor, including the thin film layer of sensing material acting as a dielectric between two parallel interdigitated electrodes. The capacitive sensor shown in Figure 4 combines a 24-fingered interdigitated electrode array with two serpentine temperature sensor devices (this design will later be cited as an example of an inefficient interdigitated electrode design). Depending on the chemical behavior of the thin film dielectric deposited over electrodes A and B and the gap between them in Figure 4(b), capacitive sensors may be constructed that detect practically any analyte in the gas or liquid phase. A representative response curve for an interdigitated electrode capacitive sensor with a polyetherurethane sensing dielectric is shown in Figure 5; the x-axis shows time in 10^3 s, the y-axis depicts change in capacitance in 10^{-12} Farads, and the underlined figures represent the partial pressures of ethanol (the analyte) in air that the sensor was exposed to in order to result in a given peak. The sharp peaks in the plot suggest the fast response time and excellent reversibility characteristic of capacitive sensors[3]. Notice that the magnitude of the measured capacitance change is directly related to the partial pressure of analyte in the sample being measured. Indeed, the capacitance of a capacitive sensor is a linear function of concentration or partial pressure of the analyte[1]. Capacitive sensors using interdigitated electrodes generally display good accuracy (1 to 2 %) over a wide range of analyte concentrations and partial pressures[2].

Figure 4: Capacitive thin-film chemical sensor[2]

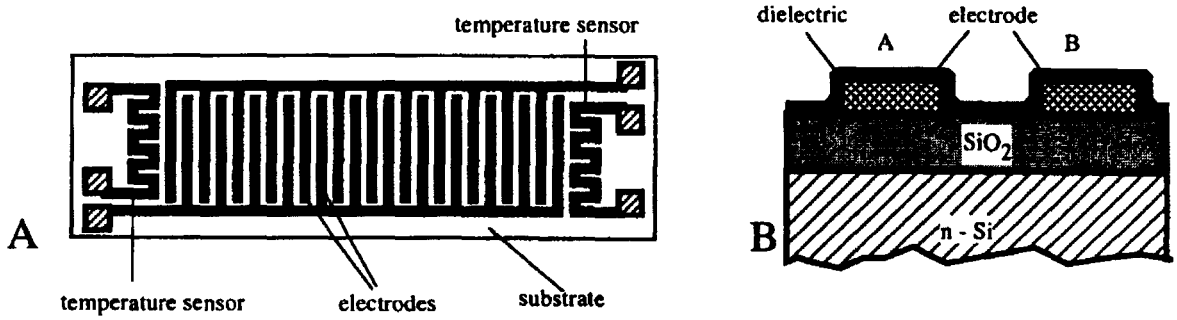
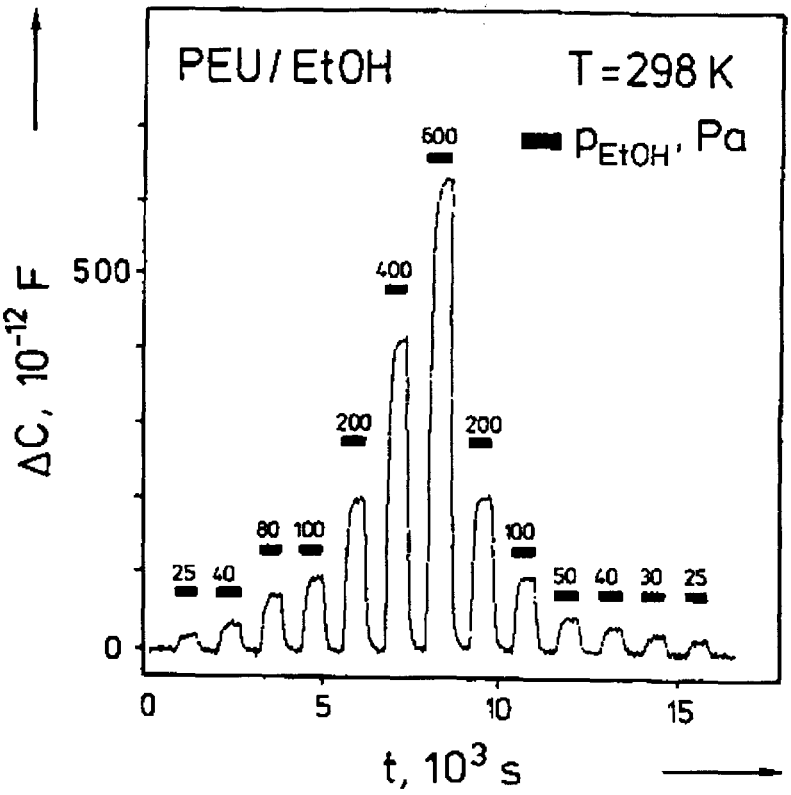


Figure 5: Response of a polyetherurethane interdigitated electrode capacitive sensor to different partial pressures of ethanol in air[1]



II.C.2 *Resistive chemical sensors.*

In contrast to capacitive sensors, which require a sensing material with very low conductivity for effective use as a dielectric, resistive sensors depend upon a flow of current through the sensing layer for an analytical measurement to be made. As the sensing layer or thin film reacts to the presence of an analyte, the conductivity of the film changes. As a result, the measured resistance through a length of the film also changes. The resistance of a resistive sensor changes as the sensor is exposed to different concentrations of analyte. As was the case with capacitive interdigitated electrode sensors, resistive interdigitated electrode sensors take advantage of the large serpentine gap area between the two interdigitated electrodes, and a resistive interdigitated electrode sensor may in turn be modeled as a chain of individual *resistors* arranged in parallel. Extraordinarily simple and elegant interdigitated electrode resistive sensors may be created. Figure 6 shows a common design for a resistive interdigitated electrode chemical sensor. As the sensing polymer films in Figure 6 react to the presence of an analyte by increasing or decreasing their conductivity, the resistance between the two interdigitated electrodes will correspondingly decrease or increase. A similar design, shown in Figure 7, shows the exact placement of the sensing layer (a hygroscopic conductive layer, in this case) over the interdigitated electrodes and the locations of two bare terminals where electrical contact with the sensor may be made. Finally, Figure 8 shows a highly-modular resistive interdigitated electrode chemical sensor design. This sensor is, again, a humidity sensor, but by changing the identity and behavior of the chemical sensing layer, a sensor for practically any analyte may be devised.

Figure 6: Resistive interdigitated electrode chemical sensor[3]

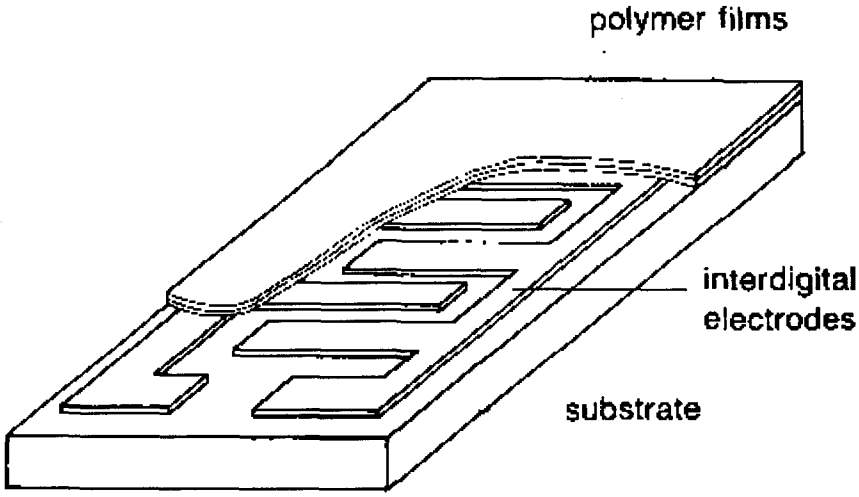


Figure 7: Resistive interdigitated electrode chemical (humidity) sensor[2]

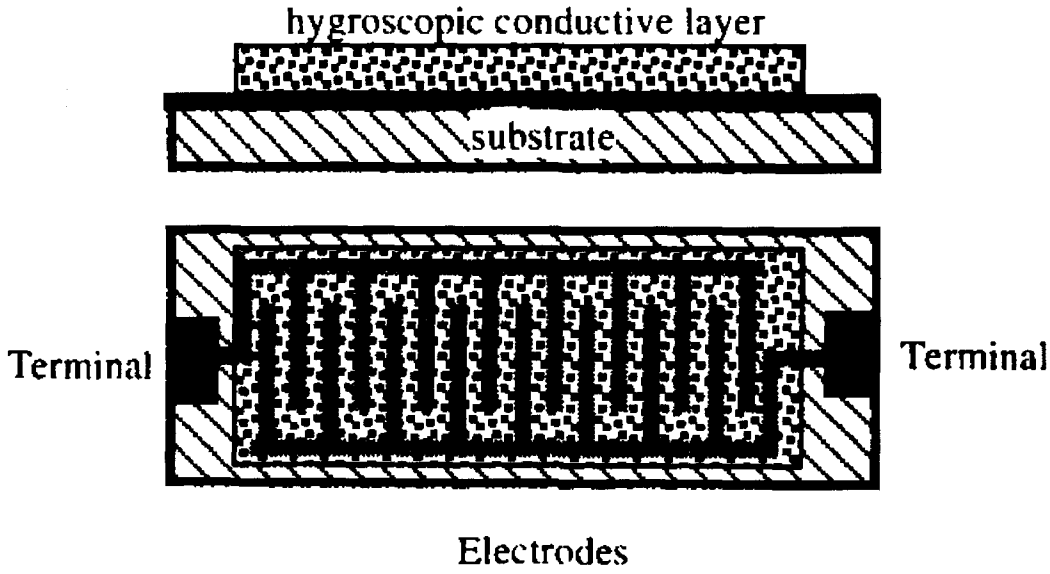
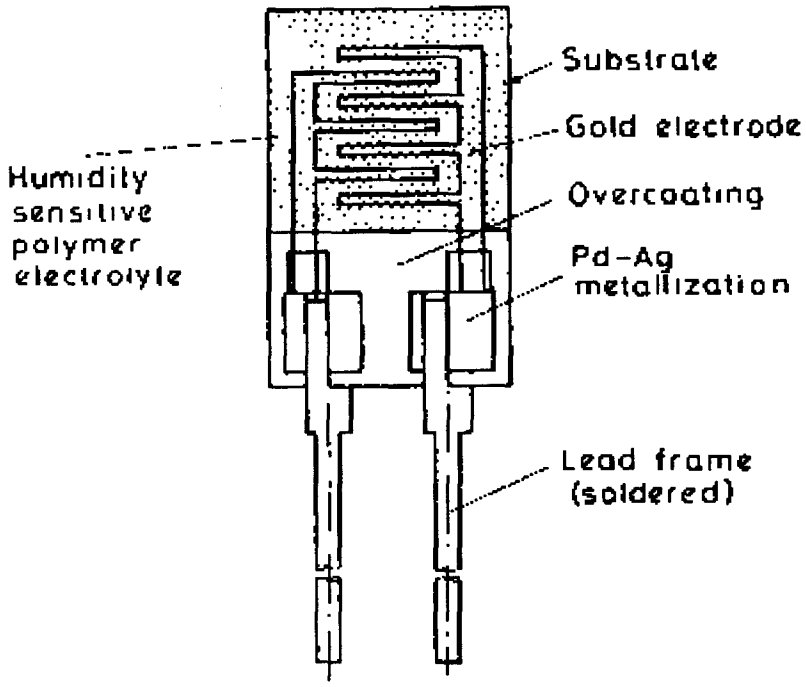


Figure 8: Modular design for resistive interdigitated electrode chemical sensor[1]

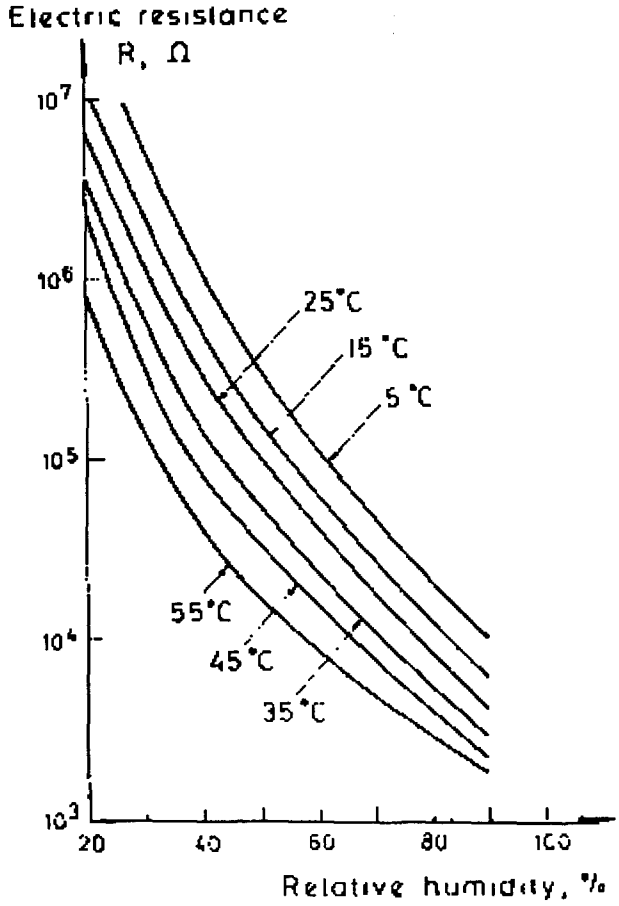


The sensor design shown in Figure 8 is a particularly useful one: it is modular (several sensors with different sensing layers could "plug into" the same device), it is small and disposable (which opens it up to several important biological and environmental applications), and it may be produced fairly cheaply. The humidity sensor in Figure 8 was characterized by A.G. Sicovend in Harsanyi[1]; the resulting plots of resistance R (in ohms) as a function of percent relative humidity at different temperatures are shown in Figure 9. Resistance changes like these span three orders of magnitude and are easy to measure reliably. The significant dependence upon temperature exhibited in Figure 9, however, necessitates the most accurate resistive interdigitated electrode sensors be integrated with temperature sensors in the same device, and several designs for integrated chemical/temperature sensor devices exist[1-3].

II.D *Surface acoustic wave (SAW) sensors.*

One additional chemical sensor often contains interdigitated electrode arrays but acts as neither a capacitive nor a resistive sensor. Surface acoustic wave (SAW) devices transmit acoustic waves through a layer of sensing material. The manner in which a sound wave propagates through a layer of sensing material is affected by the absorption of analyte molecules into the sensing layer. In general, the adsorption or absorption of analyte molecules or organisms (like bacteria) onto or into the sensing layer will *decrease* the velocity of an acoustic wave moving through the sensing layer. This decrease in acoustic wave velocity with analyte concentration is exploited by surface acoustic wave sensors. In a SAW sensor, a narrow trough in an insulating silicon substrate is lined with a thin layer of sensing material. At one end of the trough a piezoelectric oscillator

Figure 9: Resistance of sensor shown in Figure 8 as a function of relative percent humidity and temperature[1]



converts a supplied potential into an acoustic wave which travels the length of the trough. At the opposite end of the trough, another piezoelectric device acts as a receiver to convert the acoustic wave traveling in the trough back into an electrical signal. A cross-sectional diagram of a representative SAW sensor is shown in Figure 10. If an acoustic wave of constant velocity is sent through the sensing layer by the first piezoelectric device and the concentration of analyte available to the SAW device is increased, the velocity of the waves reaching the second piezoelectric device will decrease and the resulting potential produced by the second piezoelectric device will also decrease. By measuring the output potential of a SAW sensor relative to the input potential, the presence and concentration of an analyte in a gaseous or liquid phase may be detected[2,3].

Interdigitated electrode arrays play a supporting role in the operation of SAW sensors. The top-down view of a SAW sensor in Figure 11 shows that interdigitated electrode arrays drive the piezoelectric wave generators and detectors used in SAW sensors. (Note that this *differential* SAW sensor consists of not one but two separate SAW devices, one with a chemically sensitive layer (labeled "stimulus") and one without a sensing layer (labeled "reference"). This design allows the potential output from the sensor SAW device to be measured in comparison to a potential output provided by the reference SAW device). The piezoelectric devices most commonly consist of a thin film of piezoelectric material (commonly zinc oxide or aluminum nitride) deposited onto an interdigitated electrode array, as shown in Figure 11. When a potential is applied to the interdigitated electrodes, the piezoelectric material oscillates, causing acoustic waves of a known velocity to travel through the thin film of sensing material. Conversely, when these waves encounter the other piezoelectric device, the piezoelectric material vibrates,

Figure 10: Lengthwise cross-section of a surface acoustic wave chemical sensor[1]

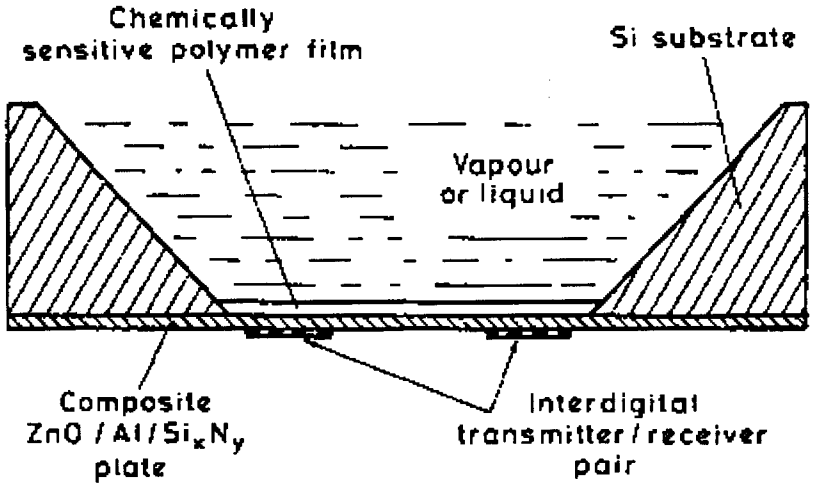
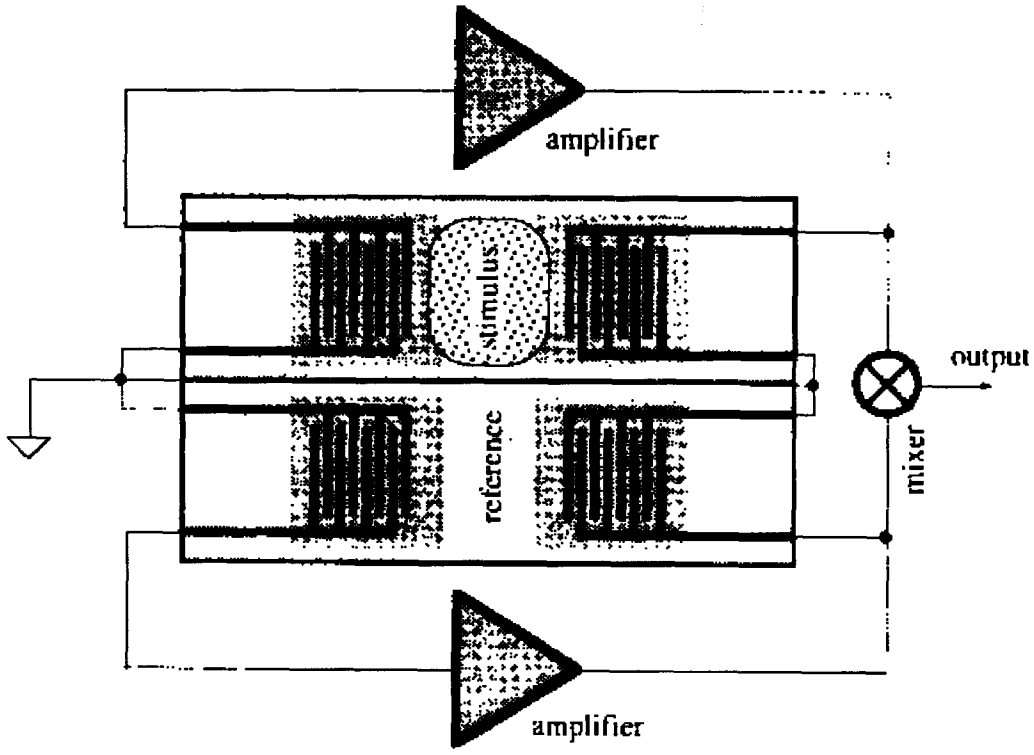


Figure 11: Top-down view of differential surface acoustic wave chemical sensor and support circuitry[2]



thereby establishing a potential difference between the two underlying interdigitated electrodes. While the use of interdigitated electrodes in SAW sensors may depart from their use in capacitive and resistive sensors, interdigitated electrodes are chosen for use in SAW devices for the same reasons they are used in other sensors: the lengthy, serpentine gap region between the two electrodes provides a large contact area between the piezoelectric material and the current that drives the oscillations of the piezoelectric material. I had the opportunity to work with SAW sensors in the past, and although SAW sensors are not explicitly studied in this work, the interdigitated piezoelectric elements of the sensors are excellent candidates for efficiency analysis by the method outlined in the next section.

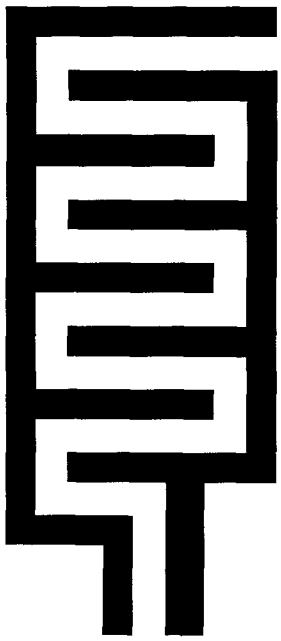
III. **Efficiency of Interdigitated Electrode Sensor Designs.**

One objective of this research is to improve upon the design of interdigitated electrode arrays in hopes of producing better sensors. Since the term "better" is relative, a precise mathematical expression for the *efficiency* of an interdigitated electrode array sensor was sought to function as an relative reference by which two interdigitated electrode designs could be compared and the better sensor of the two could be selected. However, literature searches produced no standard efficiency expression for interdigitated electrode designs. The decision was then made to devise a novel mathematical expression for the efficiency of a given interdigitated electrode sensor.

III.A *Design of the generic interdigitated electrode sensor.*

In order to devise an efficiency expression that would apply to practically any conceivable interdigitated electrode sensor, a *generic* interdigitated electrode sensor was first designed and characterized. The interdigitated electrode configuration of this generic sensor is shown in Figure 12. This generic interdigitated electrode design is quite similar to the design of many actual interdigitated electrode sensors, including those shown previously in Figures 4, 6, 7, and 8. The generic electrode serves as a template for efficiency analysis of these and practically any other interdigitated electrode. Variables are assigned to the important dimensions of the generic interdigitated electrode as shown in Figure 13. These variables are: the overall width X and height Y of the device, the electrode width E, and the serpentine gap width G. The gray area in the serpentine gap between the two interdigitated electrodes is the *sensing area* of the sensor. While sensing material is commonly deposited over the entire surface of an interdigitated electrode, only the material lying in the sensing area of the sensor actually reacts to the analyte when the device is used as a resistive or capacitive sensor. This fact is evident when the theory behind resistive and capacitive sensors is considered. In a resistive sensor, current will flow from one interdigitated electrode to the other interdigitated electrode across the serpentine gap. Essentially no current flows through the part of the sensing layer deposited directly on top of the interdigitated electrodes. As a result, the actual sensing in a resistive sensor occurs only at the serpentine gap area on the interdigitated electrode array sensor. Likewise, for a capacitive sensor, only the part of the sensing layer that lies in the serpentine gap between the two interdigitated electrodes will actually be in the dielectric zone between the two electrodes. Sensing material deposited directly on top of

Figure 12: Electrode pattern for generic interdigitated electrode sensor



the interdigitated electrodes does not function as a dielectric and does not effectively sense the analyte. As a result, the actual sensing in a capacitive sensor occurs only at the serpentine gap area on the interdigitated electrode array sensor.

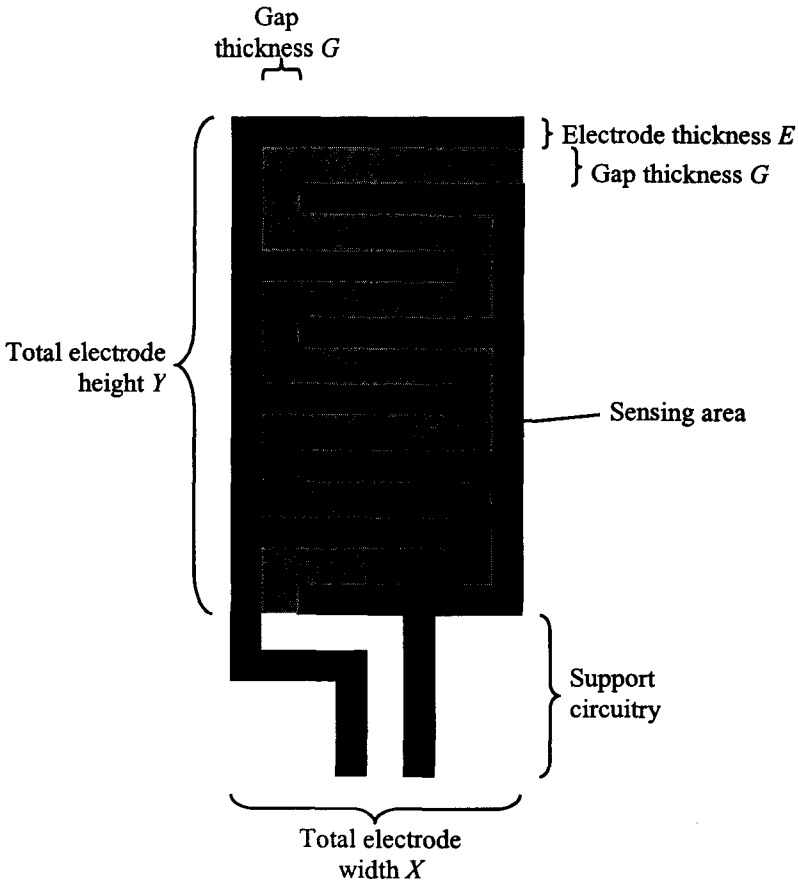
III.B *Unoptimized sensing material in the generic interdigitated electrode sensor.*

Notice that, for the generic interdigitated electrode array sensor shown in Figure 13, only a small fraction of the total sensor area actually senses the analyte. Closer examination of the design of the generic interdigitated electrode suggests that the true sensing area is actually less than we expect in Figure 13 because the width of the serpentine gap does not always remain constant. Between two parallel portions of the interdigitated electrodes, the gap width does remain constant at G, but between two electrode corners the gap width is actually greater than G. The maximum deviation from the intended gap with G corresponds to the diagonal line between a convex 90° corner on one interdigitated electrode and a concave 90° corner on the other electrode; the width of the gap between these points equals $G\sqrt{2}$ or 1.4142 G. In other words, between the electrode corners in an interdigitated electrode array, the gap width can be up to 1.4142 times greater than the gap width G between parallel electrodes.

III.C *Theory behind unoptimized sensing areas.*

Why does this increased gap width cause the sensing material between the electrode corners to remain inactive in response to analyte? Consider that the interdigitated electrode array in question finds use as a resistive chemical sensor. *Assuming that the resistance of the interdigitated electrodes is negligible*, the bulk of the

Figure 13: Definitions of important dimensions and features in the generic interdigitated electrode



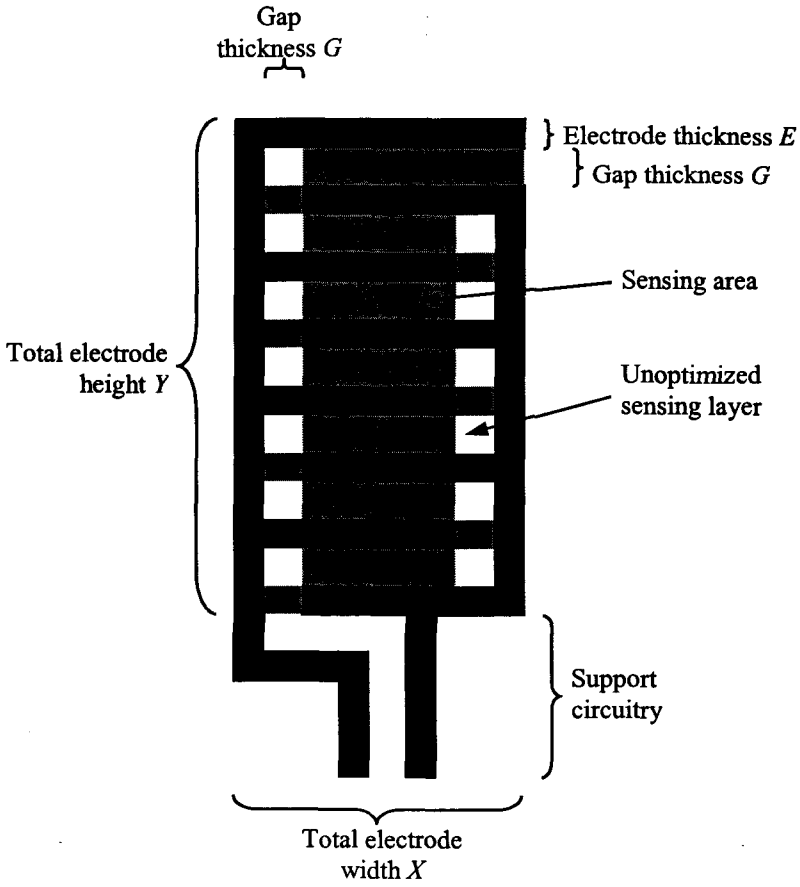
current will flow across the serpentine gap in the places where the resistance is minimal. If the resistance across the gap is proportional to G between parallel portions of the electrodes but is proportional to 1.4142 G between the corners of the electrodes, the bulk of the current will follow the low-resistance path between the parallel portions of the electrodes and only a negligible amount of current will flow across the longer diagonal path between the electrode corners. Therefore, only the regions between parallel portions of the electrodes actually function as sensors. Deleting the non-sensing regions of the serpentine gap which lie between the electrode corners, the actual sensing area of the interdigitated electrode array sensor drops even more, as shown in gray in Figure 14. Note that several of the representative designs of interdigitated electrodes previously drawn from literature (especially the designs shown in Figures 4, 6, 7, and 8) suffer from significant loss of effective sensing area in the regions between electrode corners.

III.D *Introduction of the efficiency statement for interdigitated electrode sensors.*

The analysis presented in the preceding section may be summarized in one simple statement: "Only a small fraction of the entire surface area of an interdigitated electrode chemical sensor actually is sensitive to analyte." This "small fraction" corresponds to the gray sensing region shown in Figure 14. In both a qualitative and a quantitative sense, the efficiency of an interdigitated electrode sensor may now be defined as *the ratio of the sensing area to the total area of the device.* Expressed mathematically, the efficiency ε of any interdigitated electrode chemical sensor may be defined as

$$\varepsilon = \frac{\text{Sensing area } A}{\text{Total device area } A'} \qquad (3)$$

Figure 14: Generic interdigitated array with unoptimized gap regions not included as part of the sensing area



It is evident from examining Equation 3 that the maximum possible efficiency of an interdigitated electrode array sensor would equal 1, which corresponds to a device whose entire surface area is devoted to sensing. This is unattainable in reality, however, since some support circuitry is necessary for the device, and sensing material deposited onto this support circuitry will inevitably not contribute to the total sensing area of the device.

III.E *Application of the efficiency statement for analysis and improvement of the generic interdigitated electrode sensor.*

III.E.1 *Efficiency analysis of the unimproved generic interdigitated electrode sensor.*

Equation 3 can be solved for any interdigitated electrode chemical sensor to determine a numerical efficiency ε for the sensor. By applying the definition of efficiency in Equation 3 to the generic interdigitated electrode sensor in Figure 14, formulas may be obtained that define the efficiency of *any* interdigitated electrode sensor in terms of its geometry (width X, height Y, electrode width E, and gap width G). Application of Equation 3 results in the following equation for the efficiency of the generic interdigitated electrode chemical sensor shown in Figure 14.

For the generic interdigitated electrode sensor (traditional right-angled),

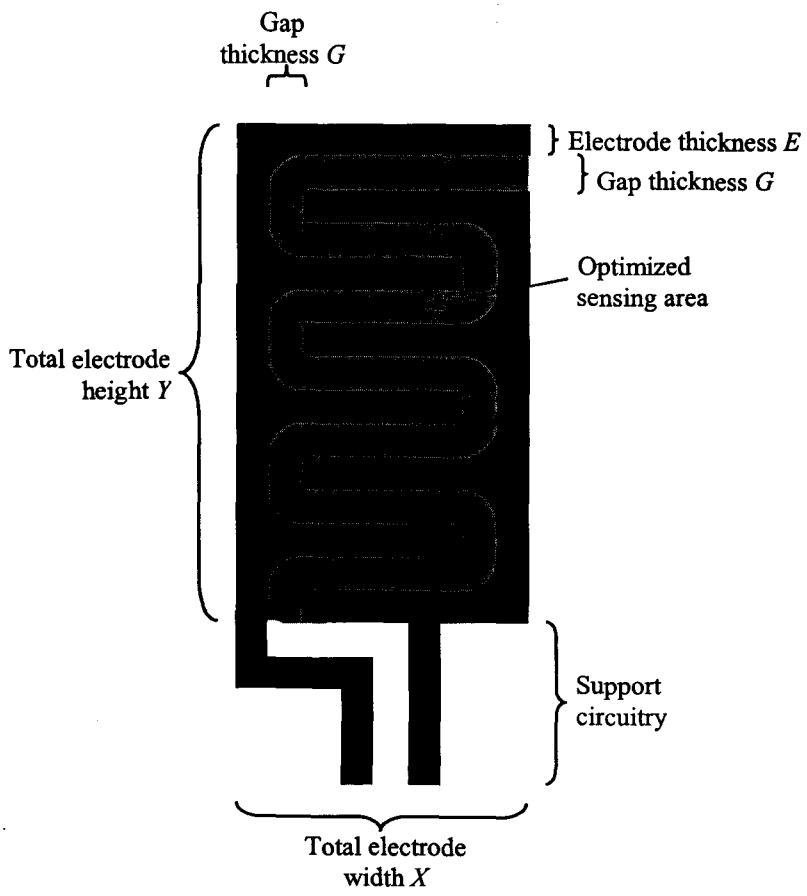
$$\varepsilon = \frac{\frac{GY}{G+E}\left(X - 2G - E\right) + G^2 + GE}{XY} \qquad (4)$$

(The underlined factor 2 in Equation 4 is called the *G*-term and will become important in later analysis of this sensor design) This expression was derived by first computing the total sensing area of the generic sensor in Figure 14 in terms of device width *X*, device height *Y*, gap width *G*, and electrode width *E*, then dividing this sensing area by the total area of the device (the product *XY*). It is relevant to note that the G^2 and *GE* terms in the numerator in Equation 4 correspond to "relics" in the determination of the total sensing area of the generic electrode; the sum $G^2 + GE$, for example, accounts for the contribution made by the small portion of sensing area in the upper right corner of the sensor in Figure 14 that extends past the sensing area present in the other six sensing areas located between parallel electrodes. These "relic" contributions to the sensing area may be safely disregarded without seriously impacting the accuracy of Equation 4, but in an attempt to keep the analysis of this generic sensor as accurate as possible, they will be retained in further calculations.

III.E.2 *Efficiency analysis of the improved generic interdigitated electrode sensor.*

The efficiency of the generic interdigitated electrode sensor shown in Figure 14, as well as the efficiency of the typical interdigitated electrode devices shown in Figures 4, 6, 7, and 8, could be improved by re-designing the interdigitated electrodes to insure a constant gap width *G* exists throughout the sensor. This may be achieved quite simply by *rounding* the concave corners in the interdigitated electrodes, as shown in Figure 15. In this interdigitated electrode device, the entire serpentine gap area is used in analyte sensing because current flows equally across the gap at all points (assuming, again, that the interdigitated electrodes themselves have no appreciable resistance). The efficiency

Figure 15: Generic interdigitated electrode sensor with curved corners to insure constant gap width throughout sensor



of the rounded corner interdigitated electrode chemical sensor shown in Figure 15 may be calculated using Equation 5; the resulting equation is

For the generic interdigitated electrode sensor (rounded corners),

$$\varepsilon = \frac{\frac{GY}{G+E}\left(X - \underline{(2-\pi/2)}G - E\right) + G^2 + GE}{XY} \qquad (5)$$

Note that this expression is identical to the efficiency expression for the ordinary 90°-cornered interdigitated electrode sensor in Equation 3 except that the underlined *G*-term has changed. For the traditional 90° corner interdigitated electrode sensor, this *G*-term is 2; for the rounded corner interdigitated electrode sensor, this *G*-term equals $(2 - \pi/2)$ or only 0.429. For both the traditional 90° corner and the rounded corner interdigitated electrode sensors, the G-term is subtracted from a positive part of the numerator in the efficiency expression, so to *maximize* the efficiency of the interdigitated electrode sensor one would *minimize* the *G*-term associated with the sensor. Rounding the 90° concave corners of a traditional interdigitated electrode sensor reduces the *G*-term from 2 to 0.429 and increases the efficiency of the sensor significantly.

III.F *Dimensional optimization of interdigitated electrode sensors.*

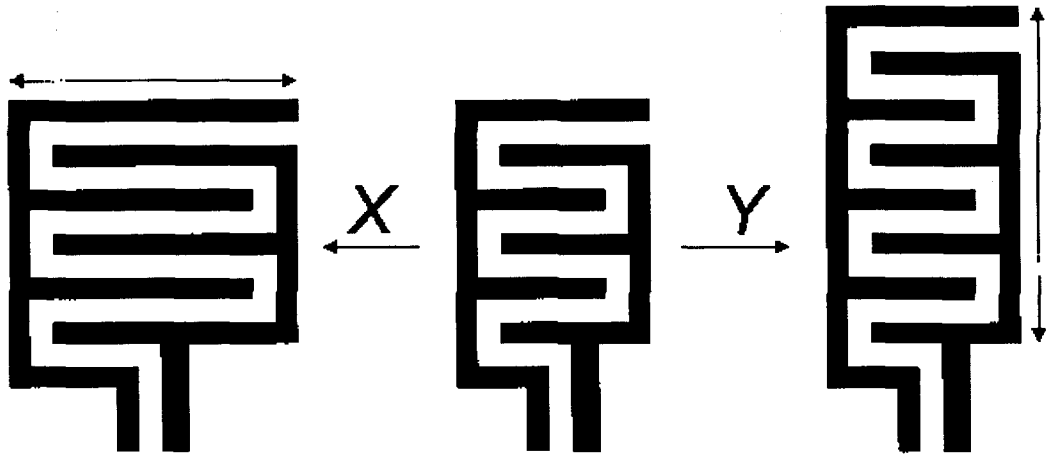
Along with rounding 90° angles within the interdigitated electrodes to improve the efficiency of the sensors, the overall dimensions of the device may be altered in an effort to maximize sensor efficiency. The problem of *dimensional optimization* seeks to determine whether an increase in sensor size in the x-dimension or the y-dimension will

result in improved efficiency for the sensor. If the generic interdigitated electrode sensor shown in Figure 14 is again adopted for analysis, an increase in electrode size in the x-dimension causes the existing interdigitated electrode "fingers" to lengthen, but no new "fingers" are added to the electrode array. If the size of the same generic sensor is increased in the y-dimension, the interdigitated electrode "fingers" remain the same length but new "fingers" are added to the electrode array. The consequences of increasing sensor size in the x- and y-dimensions are portrayed graphically in Figure 16.

III.F.1 *Dimensional optimization of the generic interdigitated electrode sensor.*

To characterize the effect of dimensional optimization on the efficiency of the generic interdigitated electrode sensor, a number of studies were conducted in which the size in one dimension of a generic interdigitated electrode sensor was kept constant while the size in the other dimension was increased. The results of the most productive of these studies are summarized in Figure 17. In the first set of data, the sensor size in the x-dimension (the length of the "fingers") is kept constant as the size in the y-dimension (number of "fingers") is increased by powers of ten. The gap thickness and electrode thickness are both held constant at $G = 1$ and $E = 0.1$ arbitrary units. As the electrode grows larger in the y-dimension and the number of "fingers" in the generic interdigitated electrode sensor increases by powers of ten, the sensing area also increases by approximate powers of ten. In other words, as the y-dimension of the sensor increases from 10 to 100 000 (a 10 000-times increase), the sensing area increases from 72.92 to 718 200 (a 9850- or nearly 10 000-times increase). The sensing area therefore increases linearly as the y-dimension size and number of "fingers" of the interdigitated electrode

Figure 16: Consequences of dimensional optimization in the generic interdigitated electrode sensor



X indicates an increase in sensor size in the x-dimension; *Y* indicates an increase in size in the y-dimension.

Figure 17: Table of results of interdigitated electrode sensor dimensional optimization

X	Y	G	E	sensing area A	total area A'	efficiency ε	$\frac{G}{G+E}$
10	10	1	0.1	72.92	100	0.7292	0.9091
10	100	1	0.1	719.3	1000	0.7193	0.9091
10	1000	1	0.1	7183	10000	0.7183	0.9091
10	10000	1	0.1	71820	100000	0.7182	0.9091
10	100000	1	0.1	718200	1000000	0.7182	0.9091
10	10	1	0.1	72.92	100	0.7292	0.9091
100	10	1	0.1	891.1	1000	0.8911	0.9091
1000	10	1	0.1	9073	10000	0.9073	0.9091
10000	10	1	0.1	90890	100000	0.9089	0.9091
100000	10	1	0.1	909100	1000000	0.9091	0.9091

The linear dimensions *X*, *Y*, *G*, and *E* have arbitrary units and the sensing and total areas have square arbitrary units; this is allowed because the efficiency ε is merely the ratio between the sensing area A and the total device area A' and is therefore unitless.

sensor increases. Since only a linear increase in sensing area is observed with increased size in the y-direction, the efficiency is observed to remain fundamentally unchanged at $\varepsilon = 0.7182$. Even though increasing the sensor size in the y-dimension increases the sensing area, it also increases the total sensor area at the same rate, so the efficiency of the original electrode is unimproved.

Now consider the second set of data, in which the y-dimension (the number of "fingers") of the generic interdigitated electrode sensor is kept constant as the x-dimension (the length of the "fingers") is increased by powers of ten. Again, the gap width G and the electrode width E are kept constant at 1 and 0.1 arbitrary units, respectively. As the existing "fingers" increase in length by powers of ten, the sensing area of the interdigitated electrode sensor increases *faster* than what would be expected by a "powers of ten" increase. In fact, as the x-dimension of the sensor increases from 10 to 100 000 (a 10 000-times increase), the sensing area of the sensor increases from 72.92 to 909 100 (a 12 470-times increase). This suggests that increasing the "finger" length of the interdigitated electrode sensor increases the sensing area of the sensor faster than can simply be explained by the increase in total sensor size afforded by increasing the x-dimension of the sensor, and the efficiency of the sensor must therefore be increasing as the x-dimension and the "finger" length of the sensor increases. Indeed, as the x-dimension of the sensor increases, the efficiency increases from an initial value of $\varepsilon = 0.7292$ to asymptotically approach a maximum value at $\varepsilon = 0.9091$.

III.F.2 *Introduction of the maximum possible efficiency.*

This last observation was initially quite surprising: the efficiency of the sensor increases as the "finger" length increases but encounters a maximum possible value, 0.9091, which neither equals nor approaches the aforementioned maximum theoretical efficiency of unity. Upon closer examination, this maximum efficiency ε_{max} was observed to equal the result when the gate width is divided by the sum of the gate width and the electrode width. Expressed mathematically,

$$\varepsilon_{max} = \frac{G}{G+E} \tag{6}$$

This equation is of paramount importance in interdigitated electrode sensor analysis. Along with the maximum *theoretical* efficiency of unity, all interdigitated electrode sensors have a maximum *possible* efficiency ε_{max} which is less than 1 and is defined to equal $G/(G+E)$. This surprising result may be understood by recalling the result of the dimensional optimization analysis: only increase in the x-dimension (the "finger" length) of an interdigitated electrode sensor will increase the efficiency of the sensor. With this in mind, consider the generic interdigitated electrode sensor introduced in Figure 14. Increasing the size of the sensor in the x-dimension will result in a sensor that is dominated by the parallel horizontal portions of the interdigitated electrodes; the small vertical portions on the left and right sides of the electrodes remain the same size and diminish in comparison to the long horizontal electrodes. For an interdigitated electrode sensor of sufficient length in the x-dimension, the tiny vertical electrodes on the left and right sides of the sensor can easily be disregarded when considering the efficiency of the

sensor. The simplified sensor now consists of n parallel horizontal electrodes of width E with $(n-1)$ gaps of width G located between electrodes. If the electrodes and gaps are l units long, then the gap area between two electrodes is $(G \times l)$ and the total gap area A over the entire electrode equals the individual gap area multiplied by the number of gaps, or $A = Gl(n-1)$. Likewise, the area of one horizontal electrode is $(E \times l)$ and the total electrode area over the entire electrode is the individual electrode area times the number of electrodes, or $n(E \times l)$. Adding the total gap area to the total electrode area results in the total area A' of the sensor, so $A' = Gl(n-1) + n(E \times l)$. Since the total gap area also equals the sensing area A of the sensor, the efficiency of the sensor may be determined by dividing the sensing area A by the total sensor area A', or

$$\varepsilon = \frac{Gl(n-1)}{Gl(n-1)+nEl} = \frac{G(n-1)}{G(n-1)+nE} \tag{7}$$

Now, if the number of horizontal electrodes n is sufficiently large, $n \cong (n-1)$ and the expression for ε in Equation 7 may be simplified to

$$\varepsilon = \frac{nG}{nG+nE} = \frac{G}{G+E} = \varepsilon_{max} \tag{8}$$

which is equivalent to the empirically-determined expression for ε_{max} in Equation 6. The ratio $G/(G+E)$ is therefore the maximum possible efficiency for any interdigitated electrode sensor with gate width G and electrode thickness E.

III.G *Introduction of the optimization term.*

Since the efficiency ε of an interdigitated electrode sensor now has both a theoretical limit ($\varepsilon < 1$) and a practical limit ($\varepsilon < \varepsilon = G/(G + E)$), ε remains a useful measure of *relative* efficiency but no longer tells how absolutely optimized a particular interdigitated electrode sensor design may be. For example, an sensor efficiency of $\varepsilon = 0.5$ is a *relatively* poor sensor, but if the particular sensor design (that is, the design dictated by gate width G and electrode width E) has a maximum possible efficiency of $\varepsilon_{max} = 0.6$, then the sensor, however relatively inefficient it may be, is well-optimized for its given design. Regardless of the efficiency of a particular sensor, if the sensor has an efficiency that is close to the maximum possible efficiency (again, dictated by the choices for G and E), then the sensor is "living up to its potential" and is well optimized. In interdigitated electrode sensor analysis there exists a need for a quantitative measurement of how well a sensor is optimized. In answer to this, the *optimization* Θ of a sensor may be defined as the ratio of the efficiency ε of the sensor to the maximum possible efficiency ε_{max} of the sensor, as shown symbolically in Equation 9.

$$\Theta = \frac{\varepsilon}{\varepsilon_{max}} \tag{9}$$

Like an efficiency measurement, the optimization Θ will be a number between zero (corresponding to a perfectly unoptimized electrode) and one (corresponding to a perfectly optimized electrode). However, unlike the efficiency ε which is further limited by the practical limit ε_{max}, the optimization Θ is not further limited by any practical

limits, and dimensional optimization of a sensor can result in a sensor with optimization Θ nearly equal to one. The optimization Θ is therefore an absolute measurement of how well an sensor with a given design (that is, a given G and E) is dimensionally optimized.

The question remains, If the efficiency ε of an interdigitated electrode is the true measure of how "good" or "bad" a sensor design is, of what use is the optimization Θ? Indeed, given a choice between an inefficient but well-optimized sensor and an efficient but poorly optimized sensor, the efficient sensor will always function as the better sensor (again, because efficiency is a relative measurement between sensors). But certain situations exist when optimization analysis, not efficiency analysis, can lead to improved interdigitated electrode sensor designs. For example, in the photolithographic preparation of interdigitated electrodes circuits, a given photolithographic instrument or process has a known resolution limit. That is, for any micropatterning operation, an absolute limit of detail exists; circuit structures can not be fabricated smaller than this absolute limit. As a result, in interdigitated electrode sensor fabrication the electrode width E and gap width G have definite minimum values, often on the order of a few microns. If minimum permissible values for E and G are set, then the minimum possible value of ε_{max} is also set. If these minimum values for E and G are used in the construction of sensors, then the efficiency of the sensor has already been effectively set to $\varepsilon = \varepsilon_{max}$ and attempts to improve the efficiency of the sensor will be fruitless. However, the opportunity still exists to maximize the optimization Θ of the sensor by conducting dimensional analysis—expanding the dimensions of the sensor in the best dimension for maximum optimization. Once the dimensions of the sensor have been optimized to their maximum permissible amounts, then the sensor can be said to have the maximum attainable

efficiency ε and optimization Θ allowable for a given photolithographic process. In this and other examples, study of sensor optimization Θ can offer valuable insight into what will (and what will not) improve the quality of a sensor design.

III.H *Efficiency and dimensional optimization as tools for sensor improvement.*

What lessons are learned from dimensional optimization of the generic interdigitated electrode chemical sensor? First, if conditions allow for an interdigitated electrode sensor to be longer in one dimension than in the other, the dimension chosen to be the longer should be the x-dimension, the dimension that defines the lengths of the "fingers." Only increasing the x-dimension will improve the efficiency of the sensor; increasing the y-dimension (the number of fingers) will not improve the efficiency of the sensor. This means that sensors such as those depicted in Figures 2, 4, 6, and 7 are *not* in their optimal configuration because they are longer in the y-direction (the number of "fingers") than in the x-direction (the length of the fingers). The efficiency of these sensors could be improved dramatically by reorienting their interdigitated electrodes so that the "fingers" run in the longest direction possible. The second "lesson" learned from dimensional optimization of interdigitated electrode sensors is that a maximum possible efficiency exists, and $\varepsilon_{max} = G/(G + E)$. Note that the maximum possible efficiency ε_{max} does not depend upon the overall dimensions (X and Y) of the sensor but instead depends only upon the thicknesses of the electrodes and the gaps between them. Therefore, if the electrode thickness E is small compared to the gap thickness G, the maximum possible efficiency ε_{max} *approaches* one. Note that this does not mean that the maximum possible efficiency can *be* one, nor does it mean that the actual efficiency of the sensor in question

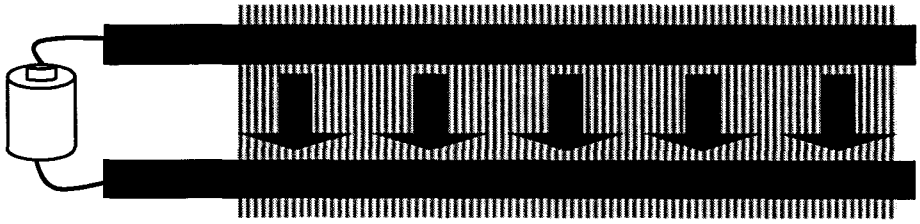
can be one, but it does mean that if the electrode thickness E is kept as small as possible, the maximum possible efficiency is highest. Construction of interdigitated electrode sensors with extremely thin electrodes can lead to several difficulties, including the limitations of photolithographic techniques discussed earlier in reference to sensor optimization Θ, so some compromise between efficiency and design constraints must usually be reached. The concepts of efficiency ε, optimization Θ, and dimensional optimization nonetheless constitute a toolbox with which the designs of many commonly-used interdigitated electrode sensors may be improved significantly.

IV. Presentation and Analysis of Novel Interdigitated Electrode Sensor Designs

IV.A *Electrodes with non-negligible resistance.*

Earlier in the discussion of interdigitated electrode sensors, the statement was made several times that the current flowing across the constant-width serpentine gap between the interdigitated electrodes is itself constant at every point in the gap *if the resistance of the interdigitated electrodes is negligible.* Essentially all commercial and experimental interdigitated electrode sensors available today adhere to this assumption, which is illustrated for the simplified case of two parallel electrodes in Figure 18. In this and the following figures the two parallel electrodes are connected to a constant current source and have a gray sensing layer deposited over them. The arrows between the electrodes represent the flow of current through the sensing layer at a particular place, and the width of a particular arrow is proportional to the current density at that point in the sensing layer. In Figure 18, the arrows nearest to the constant current source are the

Figure 18: Flow of current across a sensing layer between two parallel electrodes with *assumed* negligible resistance.



In this and subsequent diagrams the gray area represents a partially-conductive sensing layer deposited across the two electrodes. The electrodes are wired to a constant current source. The direction of the arrows represents the flow of current through the sensing layer; the thickness of the current arrows is proportional to the current density in a given region of the sensing layer.

same thickness as the arrows furthest from the current source, indicating that the current flow across the gap of constant width is assumed to be constant for every path of length *G* across the sensing layer, and the current density is likewise assumed constant at every point on the sensing layer.

If the parallel electrodes in Figure 18 have non-negligible resistances, however, the situation becomes much more complex. Ibl[4] examines in depth the complications that arise when the finite conductivity of an electrode is addressed. The negligible-resistance approximation for electrodes is no longer true

> in the electroplating of thin wires, in the deposition of thin coatings on an insulating substrate, or for certain electrodes made of poorly conducting materials. If the current is fed to the ends of the electrode there is within the latter an ohmic potential drop, so that the metallic side of the electrode-solution interface is no longer an equipotential surface.[4]

The validity of Ibl's statement when applied to interdigitated electrode sensors merits some analysis. First, thin conductive coatings on an insulating substrate and electrode materials with measurable resistances are all routinely used for the fabrication of interdigitated electrodes. Electrodes made by vapor deposition of metal atoms on an insulating substrate inevitably have resistances associated with them. Likewise, electrodes created by depositing a pattern of conductive material (such as conductive epoxy) onto an insulating substrate also have considerable internal resistances, as the author discovered in his own research. In short, only in rare cases can one assume that

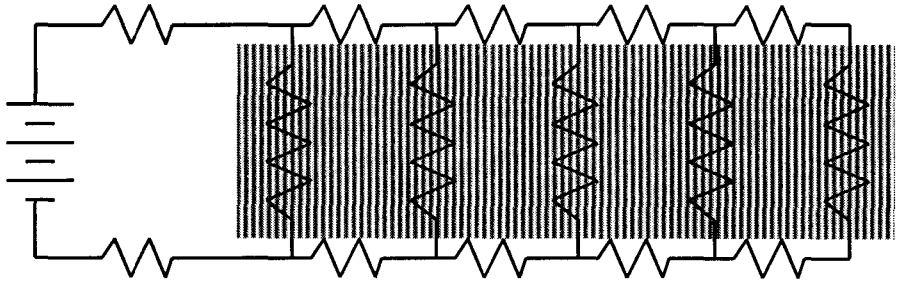
the entire surface of an electrode is at the same potential (rare cases would include electrodes made of solid conductors, but these are rarely encountered in interdigitated applications). Thus, as Ibl claims, one must assume that a potential *gradient* exists along an electrode with a non-negligible resistance.

IV.B *Circuit model of parallel electrode chemical sensor.*

In order to study the complex distribution of current in a parallel electrode chemical sensor where the resistance of the electrodes is significant, Ibl and many others have modeled the sensor as a simple electric circuit consisting of resistors connected to a constant current source. This models the behavior of a resistive sensor; a capacitive sensor could be modeled using capacitors arranged in much the same manner. My own interpretation of this circuit model is shown in Figure 19. In this diagram, the sensing area is still represented as a gray rectangle superimposed over the circuit. The parallel electrodes are represented by the two horizontal lines of resistors in series, and the resistance across the sensing layer is represented by the number of vertical resistors that connect the two parallel electrodes at various points along their lengths. Notice that the resistance per unit length of the electrodes remains constant (hence the resistors that make up the electrode are of equal resistance), and the resistance across the sensing layer is also constant (hence the resistors that bridge the sensing layer are of equal resistance).

The circuit shown in Figure 19 may now be analyzed with respect to current distribution and current flow through the circuit. Consider current flowing in a clockwise fashion, originating at the upper (+) terminal of the constant current source and traveling through the first "electrode resistor" on the left of the upper horizontal series of resistors

Figure 19: Circuit model for current flow in parallel electrode chemical sensor



In this diagram, the gray rectangle represents a sensing layer deposited across two parallel electrodes, each of which is represented by a horizontal series of resistors. The resistance across the sensing layer itself is represented by the number of vertical resistors that lie underneath the gray sensing layer and connect the two electrodes at several points along their length.

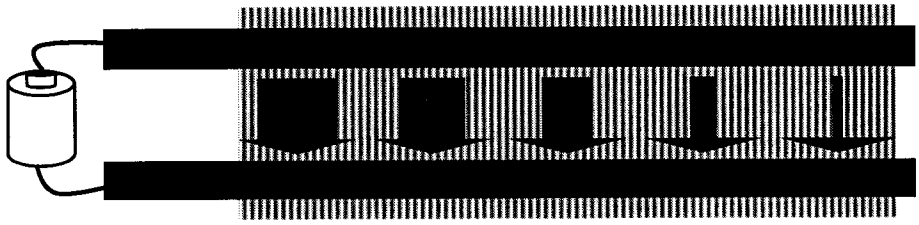
that models one of the electrodes. As the full current produced by the source passes through this resistor and reaches the beginning of the sensing layer, some of the current will branch off at this junction and flow through the sensing layer, to the other electrode, and back to the current source. However, since the resistance across the sensing layer is assumed to be greater than the resistance along the electrode, the bulk of the current continues to flow down the electrode. After traveling an arbitrary distance down the electrode, another junction is encountered. A slightly smaller current is flowing into this junction than was flowing into the previous junction, so a slightly smaller amount of current will flow across the sensing layer. Again, the majority of the current (a slightly smaller amount of current) will proceed down the electrode. As this process is repeated over a large number of junctions, the current actually continuing down the electrode grows smaller and smaller until, at the extreme end of the electrode, the small remaining current all flows across the sensing layer and into the other electrode. At this electrode, the opposite of current distribution has been occurring. As we travel along the second electrode and proceed toward the current source, the number of junctions feeding current into the electrode increases. By the end of the sensing layer and right before the negative input of the current source, all the current distributed into the circuit has been returned to the second electrode.

If the preceeding circuit model for a parallel electrode chemical sensor is true, then the amount of current flowing along the two electrodes (the current density at various points along the electrodes) grows smaller farther from the current source and grows larger closer to the current source. As a result, the portion of the sensing layer nearest to the current source has the largest flow of current across it, and the portion of

the sensing layer at the extremities of the sensing layer (the portion farthest from the current source) has the smallest amount of current flowing across it. Figure 20 attempts to visually portray this gradient current flow along the sensing layer. Nearest to the current source, the thick arrow indicates that the largest amount of current is flowing across the sensing layer at this point. Farthest from the current source, the thin arrow indicates that the smallest amount of current is flowing across the layer at this point. Phrased another way, Ibl's assertion that a potential gradient exists along the electrodes means that, according to Ohm's law, if the resistance across the sensing layer remains constant, then the current flowing across the layer must vary along the length of the layer.

One might now be tempted to ask, What is the significance if the current flow across the sensing layer is not constant at every point? Irregular current flow across a sensing layer is a serious and significant threat to sensor efficiency and integrity. If the portion of the sensing layer nearest to the current source receives the largest current flow, then this section of the sensor will be most sensitive to the detection of analytes. At the extremities of the sensor, however, where the sensing layer receives the smallest current flow, the sensing material may react to the presence of analyte but the flow of current through the sensor will be largely unaffected by this reaction. Therefore, detection of analyte at the extremities of a resistive sensor will produce a much lower signal than the detection of an equal concentration or amount of analyte at the end closest to the current source. This irregular sensing pattern is highly undesirable; it places excessive importance on the part of the sensor closest to the current source and effectively does not use the part of the sensor farthest from the current source. Another concern addresses the relatively large current that flows across the portion of the sensing layer located closest to

Figure 20: Flow of current across a sensing layer between two parallel electrodes with *non*-negligible resistance



The different thicknesses of the arrows across the sensing layer indicate the relative amount of current (the current density) flowing across the sensing layer at that point.

the current source. This current could easily exceed the expected values for current flow across the sensing layer (particularly if the expected values were generated using a "zero-resistance electrode" model), and electrolytic or thermal decomposition of the sensing layer at this point could occur. In short, whether in a simple parallel electrode sensor or a complex interdigitated electrode sensor, constant current flow across all points along the sensing layer is always desired. However, if the traditional constant-gap-width electrode design is used and if the electrodes themselves possess a non-negligible resistance, the goal of constant current flow across the gap will remain unrealized.

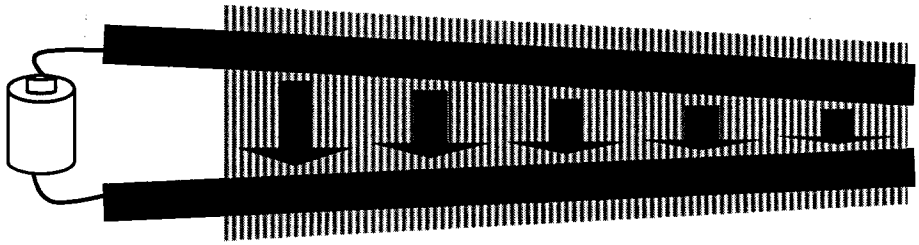
IV.C *The tapered gap.*

The author devised a novel solution to the problem of variable current flow across the sensing layer along the length of a sensor. Recall that Ohm's law was previously applied to the traditional constant-gap-width electrode design as follows: if the potential along an electrode is variable and current from the electrode flows across a constant resistance, the current flowing across that resistance will be variable. In specific, the current across the constant-resistance sensing layer (gap) will increase as we approach the current source and decrease as we move away from the current source. It is obvious in this analysis that holding one variable in Ohm's law constant allows the other two to be mutually variable: holding the gap resistance across the sensing layer constant requires the current to change as the potential changes. Since one would prefer the current flow across the sensing layer to remain constant, consider Ohm's law with constant current. As the potential varies, the *resistance* must also vary. In particular, the resistance would have to increase as we approach the current source and decrease as we move away from

it. Since the resistivity (roughly, the resistance per unit length) of the sensing layer is constant, a range of variable resistances along the length of the sensor may indeed be accomplished by *tapering* the sensors, angling them slightly towards each other and reducing the gap thickness at the extremities of the sensor. Figure 21 the current-magnitude arrows to convey this concept. The constant thickness of the arrows in Figure 21 indicates that the current flow between the tapered electrodes and across the sensing layer remains constant throughout the length of the sensor. Consider the end of the sensing layer closest to the current source, where the potential difference between the electrodes is the highest (and, previously, the highest current flowed). This large potential difference encounters a similarly-large resistance (large gap width) across the sensing layer, and a small amount of current flows across the sensing layer. At another point arbitrarily far down the electrode, the slightly diminished current encounters a junction with a slightly diminished resistance (a slightly shorter gap width). With both the potential and the resistance diminished by the same factor, by Ohm's law the current flowing across the sensing layer at this point will be *the same* as the current flowing across the sensing layer at the first point. Finally, at the extremities of the electrode where the smallest current is available to flow across the sensing layer, the smallest gap width and smallest resistance across the layer is encountered, so again the constant current flow across the gap is maintained.

The tapered gap improvement is not limited to simple sensors consisting of two straight electrodes. Interdigitated electrode sensors could easily be constructed with gaps that taper linearly as the distance from the current source increases. The current thrust of

Figure 21: Constant current flow across the sensing layer in a *tapered gap* parallel electrode sensor



The constant thickness of the arrows indicates that the current flow between the tapered electrodes and across the sensing layer remains constant throughout the length of the sensor.

this research lies in the creation and efficiency testing of interdigitated electrode sensor designs that feature the tapered gap improvement.

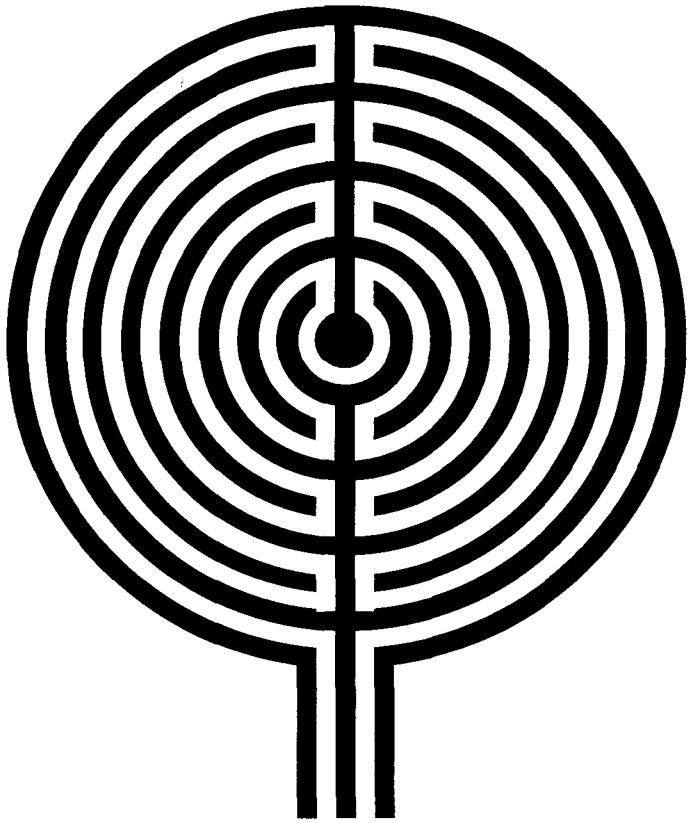
IV.D *Novel interdigitated electrode sensor designs.*

A sidelight to my interdigitated electrode efficiency research has been the design (and, in some cases, fabrication and testing) of novel interdigitated electrode chemical sensors for particular applications. Two representative novel designs, the circular interdigitated electrode sensor and the hexagonal array interdigitated electrode sensor, will be presented and briefly commented upon.

IV.D.1 *Circular interdigitated electrode sensor.*

During research related to this work at Pacific Northwest National Laboratory in Richland, Washington, I realized the need for interdigitated electrode sensor designs in shapes other than squares and rectangles. Automated fluid deposition, for example, is an industrial technique in which a computer-programmable robot arm uses a needle-tipped syringe to dispense tiny dots of material onto devices such as electronic components. Automated fluid deposition systems are well-suited for the assembly-line deposition of sensing layers onto interdigitated electrode sensors (as well as other sensors[5]), but the dispensed layers take the form of dots. These dots either fail to cover the entire gap area of rectangular interdigitated electrode or flood beyond the gap area, thereby wasting sensing material. A circular interdigitated electrode is better suited to receive automatically-dispensed circular sensing layer dots. My prototype design for a circular interdigitated electrode is shown in Figure 22. Note that this circular interdigitated

Figure 22: Circular interdigitated electrode sensor design

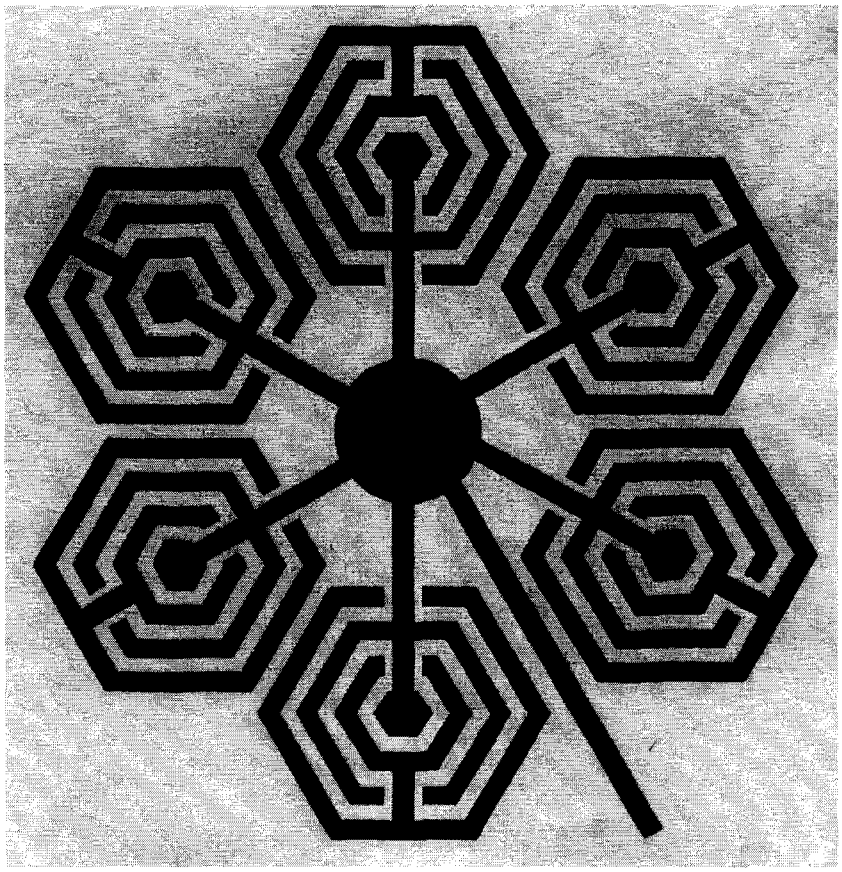


electrode sensor design suffers from the same 90° electrode corners that were discussed earlier, so some efficiency improvements remain to be made. The design would be a good choice of interdigitated electrodes for use with a circular sensing layer such as that dispensed by automated fluid deposition.

IV.D.2 *Hexagonal array interdigitated electrode sensor.*

The second novel interdigitated electrode sensor design addresses a common issue in sensor development. Often, one sensing material will not be sufficiently selective to accurately determine the constituents of a complex mixture of analytes. More realistically, sensing layers are developed that are sensitive only to one compound or one class of compound. The ability to sense several analytes simultaneously then rests on the integration of *many* of these individual sensing elements into the same sensor device. Silicon chips with 100 or more small interdigitated electrode sensors have been constructed for this purpose; with different sensing materials on each sensor, such a chip would be sensitive to a broad range of analytes. Sensor devices that make use of these chips must be of reasonable size, however, so the size of these sensing arrays must be kept as small as possible. Since hexagonal sensors would pack more densely onto the surface of a chip than ordinary square or rectangular sensors would, an hexagonal array sensor was devised for this purpose. A diagram of the sensor is shown in Figure 23. In an effort to reduce the number of wire connections required for this sensing chip, one of each sensor's two interdigitated electrodes are mutually connected to a single output wire (ground). Each sensor's remaining interdigitated electrode is connected to an individual

Figure 23: Hexagonal array interdigitated electrode sensor



output wire. Such an array of seven sensors has only eight input/output connections, a considerable improvement over the 14 connections that would otherwise be required.

References

1) Harsanyi, G. *Polymer Films in Sensor Applications: Technology, Materials, Devices and Their Characteristics*; Technomic Publishing Company: Lancaster, Pennsylvania, 1995.

2) Fraden, J. *Handbook of Modern Sensors*; American Institute of Physics: Woodbury, New York, 1997.

3) Hauptmann, P. *Sensors: Principles and Applications*; Prentice Hall International: Hertfordshire, UK, 1991.

4) Ibl, N. *Current Distribution,* in *Electrodics: Transport*; Yeager, E., Ed.; Plenum Press: New York, 1983; Vol. 6.

5) Domansky, K.; Rose, A.; Grover, W. H.; Exharos, G. J. *Materials Science and Engineering B*, in press.

6) Ferris, C. D. *Introduction to Bioelectrodes*; Plenum Press: New York, 1974.